Spin Pumping in the Presence of Spin-Orbit Coupling

Kai Chen and Shufeng Zhang*
Department of Physics, University of Arizona, Tucson, Arizona 85721, USA
(Received 20 October 2014; published 26 March 2015)

Spin pumping and related phenomena have been observed recently in heavy metals and topological insulators, where the spin-orbit coupling plays an essential role. We have developed a spin-pumping formalism that explicitly includes the spin-orbit coupling at interfaces and disorder in the layers. Spin pumping across an interface with spin-orbit coupling and the attendant backflow are treated on an equal footing. We resolve some long-standing issues on the conflicting conclusions about the spin-diffusion length for Pt, and the origin of spin-memory loss at interfaces with heavy metals. In addition, we predict some heretofore unanticipated spin-pumping phenomena.

DOI: 10.1103/PhysRevLett.114.126602 PACS numbers: 72.25.Mk, 73.40.-c

Spin pumping refers to the phenomenon in which a precessing magnetic layer emits a spin current to the surrounding nonmagnetic (NM) metallic layers. Since its first demonstration a decade ago in conventional transition-metal multilayers [1], experiments on spin pumping have been extended to topological interfaces [2,3], magnetic insulators [4], heavy metals [5–11], and semiconductors [12–14]. Theoretical analyses of these experiments usually use scattering theory [15] in which the spin current $\mathbf{j}^s$ near the interface is given by the mixing conductance,

$$\mathbf{j}^s = \frac{\hbar}{4\pi}\left(g_r \mathbf{m} \times \frac{d\mathbf{m}}{dt} - g_i \frac{d\mathbf{m}}{dt}\right). \quad (1)$$

Here $\mathbf{m}$ is a unit vector representing the precessing magnetization, g_r and g_i are the real and imaginary parts of the mixing conductance $g \equiv g_r + ig_i = \sum(1 - r_\uparrow r_\downarrow^*)$ where r_σ is the reflection coefficient for the spin $\sigma = \uparrow, \downarrow$ at the interface between NM and magnetic layers.

The conventional theory has been able to explain general features of spin pumping experiments, such as the enhancement of the Gilbert damping for thin films and the charge voltage induced by spin pumping. However, some glaring omissions of the above formalism are the effects of disorder, and more importantly the spin-orbit coupling (SOC) at interfaces. In recent experiments the focus has been on spin pumping in new materials, e.g., a topological insulator (TI) in contact with a precessing ferromagnet [2], where the physics is dominated by SOC at the interface. The mutual dependence in SOC systems between the momentum and spin of conduction electrons means that the spin current is described by two vectors; i.e., the momentum (the net flow direction of electrons) and spin polarization (the average spin direction) depend on the degree of momentum-spin locking by the SOC. In the case of spin pumping, electrons pumped from the precessing magnet pass an interface layer in which the SOC can absorb, rotate, and flip the electron's spin; therefore the interface dictates the resulting spin current in the NM layer. It follows that the spin accumulation induced in the NM layer creates a diffusive spin current which is altered by the presence of SOC at the interface; in addition, the "backflow" [16] has to be reformulated on an equal footing to that outlined above for interfaces with SOC.

Experimentally, the influence of SOC at interfaces on spin-dependent transport has been recognized as early as a decade ago. Giant magnetoresistance (GMR) studies on Cu/Pt multilayers in the current-perpendicular-to-plane (CPP) geometry indicated that there must be a significant spin-memory loss at interfaces between Cu and Pt layers so as to consistently explain the large amount of experimental data [17]. To our knowledge, to date no attempt has been made to explain such a large spin-memory loss. Other examples are the observation of spin-transfer torque in a FM/Pt (FM = Co, NiFe, CoFeB) bilayer for which the physical origin remains hotly debated [18–20], and spin-pumping experiments in NiFe/Pt by several groups which have led to a controversy regarding the spin-diffusion length in Pt; estimates range from a few to a hundred monolayers [6–11]. The origin of these controversies may be due to the omission of the SOC at interfaces in the theories used to analyze the experiments. Also, the novel phenomena observed at the interface between topological insulator and NM layers [2] cannot be explained by the present theory.

In this Letter, we provide a derivation for spin pumping in the presence of SOC at interfaces and with arbitrary disorder both in the FM and NM layers. It should be noted that the previous theory used a scattering formalism approach where the spin current is expressed in terms of reflection coefficients at interfaces. Reflection and transmission coefficients are most useful for calculating transport in mesoscopic conductors; however, they are inconvenient and prohibitively complicated for diffusive systems due to the presence of a large number of transverse scattering paths [21]. Here we adopt a more conventional method, i.e., the linear response approach within the adiabatic approximation where the spin-pumping conductivity is related to a set of conventional Green's functions for which disorder can be

included explicitly. We apply the formalism to address qualitative as well as quantitative aspects of recent experiments, and predict new phenomena.

Spin-pumping formalism.—Consider a FM/NM bilayer in which the magnetization of the magnetic layer is spatially uniform and precessing around a direction $\hat{\mathbf{m}}_0$ such that $\mathbf{m}(\mathbf{r},t)=\mathbf{m}_0+\delta\mathbf{m}(\mathbf{r},t)$. The interaction between the spin of an itinerant electron and the magnetization is modeled by the conventional exchange interaction, $V(\mathbf{r},t)=-J_{\rm ex}\boldsymbol{\sigma}\cdot\mathbf{m}(\mathbf{r},t)$. By using the Kubo formalism [22], the spin-current density tensor, $\mathbf{j}_i^\alpha(\mathbf{r},t)$, where i denotes the direction of transport and α the direction of spin polarization, is given as

$$j_i^\alpha(\mathbf{r},t)=\frac{iJ_{\rm ex}}{2}\sum_{\beta=x,y}\int d^3r'\int dt'\Theta(t-t') \times\langle[\mathcal{J}_i^\alpha(\mathbf{r},t),\mathcal{S}^\beta(\mathbf{r}',t')]\rangle\delta m_\beta(\mathbf{r}',t'), \quad (2)$$

where $\mathcal{S}^\beta(\mathbf{r}',t')$ and $\mathcal{J}_i^\alpha(\mathbf{r},t)$ are the spin-density and spin-current-density operators.

In the above equation the retarded response function is evaluated by using the Mastubara frequency representation. In the Supplement Material [23], we show that the spin current can be cast into the following compact form,

$$j_i^\alpha(\mathbf{r},t)=\frac{\hbar}{4\pi}\frac{J_{\rm ex}\hbar^2}{2m_e i}\sum_\beta\int_{\rm FM}d^3r' \times{\rm Tr}[\sigma^\alpha G^R(\mathbf{r},\mathbf{r}';E_F)\overleftrightarrow{\partial}_i\sigma^\beta G^A(\mathbf{r}',\mathbf{r};E_F)]\frac{dm_\beta}{dt}, \quad (3)$$

where $G^{A/R}(r,r';E_F)$ is the retarded or advanced 2×2 spinor Green's function and $\overleftrightarrow{\partial}_i$ the antisymmetric differential operator.

While the above spin-pumping current density is general, its usefulness relies on the proper determination of the position and spin-dependent retarded Green's function for specific systems. The simplest example is a spin-conserving system where the Green's function is diagonal with respect to the magnetization vector, i.e.,

$$G(\mathbf{r},\mathbf{r}')=\frac{g_\uparrow(\mathbf{r},\mathbf{r}')+g_\downarrow(\mathbf{r},\mathbf{r}')}{2}+\frac{g_\uparrow(\mathbf{r},\mathbf{r}')-g_\downarrow(\mathbf{r},\mathbf{r}')}{2}\boldsymbol{\sigma}\cdot\mathbf{m}, \quad (4)$$

where $g_\uparrow(\mathbf{r},\mathbf{r}')$ and $g_\downarrow(\mathbf{r},\mathbf{r}')$ are the Green's functions for the electron with spin parallel or antiparallel to the magnetization. For clarity, we use capital G for spinor Green's functions and lowercase g for scalar Green's functions. By inserting Eq. (4) into Eq. (3), we find

$$\mathbf{j}_i(\mathbf{r},t)=\frac{\hbar}{4\pi}\left[\Gamma_i^{re}(r)\mathbf{m}\times\frac{d\mathbf{m}}{dt}-\Gamma_i^{im}(r)\frac{d\mathbf{m}}{dt}\right], \quad (5)$$

where the spin-pumping coefficient is $\Gamma_i(\mathbf{r})=\Gamma_i^{re}(\mathbf{r})+i\Gamma_i^{im}(\mathbf{r})$, and

$$\Gamma_i(\mathbf{r})=\frac{J_{\rm ex}\hbar^2}{m_e}\int_{\rm FM}d^3r'g_\uparrow^R(\mathbf{r},\mathbf{r}')\overleftrightarrow{\partial}_i g_\downarrow^A(\mathbf{r}',\mathbf{r}). \quad (6)$$

Equation (5) reproduces the spin-pumping formalism, Eq. (1), except that in the present formulation we express the spin-pumping conductivity in terms of retarded and advanced Green's functions rather than reflection coefficients. In the limiting case where there is no disorder, the Green's functions are directly related to the reflection coefficients. As we have shown in Ref. [23] (see Sec. S2), the spin-pumping coefficient defined above reduces to the mixing conductance in this limit. One advantage of expressing spin pumping by using Green's functions is that the effect of the spin-independent disorder can be readily included, as we show in Ref. [23] (see Sec. S4). Note that the imaginary part in Eq. (5) is much smaller than the real part [28]; we will discard it thereafter.

One application of the present work is to evaluate spin pumping in the presence of the SOC interface; in this case the spinor Green's functions are not diagonal in spin space. We consider an interfacial Rashba spin-orbit coupling of the standard form,

$$V(\mathbf{r})=\alpha_R\delta(z)(\hat{\mathbf{k}}\times\hat{\mathbf{z}})\cdot\boldsymbol{\sigma}, \quad (7)$$

where α_R denotes the Rashba coefficient. There are two essential approaches to include the above Rashba potential in the Green's functions. First, we could introduce an additional term for the boundary condition of the Green's function; i.e., the derivative of the Green's function would have a jump across the interface, similar to Eq. (S15) for a δ potential in Ref. [23] (see Sec. S2). Matching boundary conditions that entail rotation of spinor Green's functions makes this approach tedious and difficult. An alternative is to treat the Rashba interaction as a perturbation such that the Green's function can be readily obtained as long as we have the Green's function in the absence of the Rashba term. We find the latter approach is simpler and valid up to second order in the Rashba potential. The Green's function may be obtained via Dyson equation [22], $G(\mathbf{r},\mathbf{r}')=G^0(\mathbf{r},\mathbf{r}')+\int d^3r_0G(\mathbf{r},\mathbf{r}_0)V(\mathbf{r}_0)G(\mathbf{r}_0,\mathbf{r}')$, where G^0 is the Green's function without the spin-orbit coupling. After some cumbersome algebra we find to second order in the Rashba coefficient [see details in Ref. [23] (Eq. S5)] the spin current near the interface can be written in compact form as

$$\mathbf{j}_z(0^-)=\frac{\hbar}{4\pi}\frac{J_{\rm ex}^2}{J_{\rm ex}^2+\Delta^2}\Gamma^0\mathcal{A}_1\cdot\left(\mathbf{m}\times\frac{d\mathbf{m}}{dt}\right), \quad (8)$$

at the FM side of the interface, and

$$\mathbf{j}_z(0^+)=\frac{\hbar}{4\pi}\frac{J_{\rm ex}^2}{J_{\rm ex}^2+\Delta^2}\Gamma^0\mathcal{A}_2\cdot\left(\mathbf{m}\times\frac{d\mathbf{m}}{dt}\right) \quad (9)$$

for the NM layer side of the interface. Here Δ is the imaginary part local self-energy due to disorder, Γ^0 the spin-pumping conductivity across the interface without disorder, which is the same as the "mixing conductance" in the scattering formalism, and the matrices $\mathcal{A}_1$ and $\mathcal{A}_2$ are

$$\mathcal{A}_1 = \begin{pmatrix} 1 & 0 & 0 \\ 0 & 1 & 0 \\ 0 & 0 & 1+\eta \end{pmatrix};$$

$$\mathcal{A}_2 = \begin{pmatrix} 1-2\eta & 0 & 0 \\ 0 & 1-2\eta & 0 \\ 0 & 0 & 1-3\eta \end{pmatrix}.$$

where $\eta = (\alpha_R k_F/E_F)^2$. From *ab initio* calculations the Rashba coefficient has been estimated to be between 0.03 and 3 eV Å for different systems [29]. Given that the Fermi vector k_F is of the order of an inverse angstrom, η is as large as 0.3 for the systems to be discussed below.

The physical meaning of the diagonal matrices $\mathcal{A}_1$, $\mathcal{A}_2$ is as follows: without SOC at the interface the spin current is polarized in the direction of $\mathbf{m} \times d\mathbf{m}/dt$ throughout the structure; the Rashba term at an interface makes the spin of the electron rotate about the axis $\hat{z} \times \hat{\mathbf{k}}$ [see Eq. (7)]. Since this direction is in the plane of a layer, spins polarized parallel and perpendicular to the plane of the layers receive different torques; thus $\mathcal{A}_1$ and $\mathcal{A}_2$ are not unit matrices. However, the matrices remain diagonal because the off-diagonal terms vanish after summing over the momentum of conduction electrons. In $\mathcal{A}_2$, $1-2\eta$ and $1-3\eta$ refer to the spin-memory loss factor for spin currents flowing across the interface that are polarized parallel and perpendicular to the interface.

Having determined the spin-pumping current near an interface, we evaluate the backscattering or backflow of the spin current that reduces the current arising from spin pumping. Consider a boundary condition such that the spin current is zero at the outer boundary of the NM layer; then one can write the spin current in the layer in terms of its value at the interface, i.e., $\mathbf{j}_z(z>0) = \mathbf{j}_z(0^+)\sinh[(t_N - z)/\lambda_{\rm sd}]/\sinh(t_N/\lambda_{\rm sd})$, where $\lambda_{\rm sd}$ is the spin-diffusion length. Consequently, a spin accumulation $\boldsymbol{\mu}$ is established in the NM layer; this accumulation is polarized transversely to the magnetization of the FM layer. For this reason the spin current backscattered into the FM layer is also polarized transversely to the magnetization of the layer, and decays within a spin-coherence length, which for a strong ferromagnet such as Co and Fe is a few monolayers [30], The ensuing difference between spin accumulations in the NM and FM layers creates a bias which drives a diffusive spin-current flow towards the FM layer known as the backflow due to spin pumping [16]. In previous approaches without SOC, backflow was accounted for by introducing the mixing conductance across the interface. Here, we include backflow by using Eq. (3) where the source term, the magnetization dynamics in the FM layer, is replaced by the spin accumulation $\boldsymbol{\mu}(\mathbf{r})$ in the NM layer, i.e.,

$$j_z^{\alpha,\rm back}(\mathbf{r}) = \frac{\hbar}{2m_e i C}\sum_\beta \int_{\rm NM} d^3\mathbf{r}' \times {\rm Tr}[\sigma^\alpha G^R(\mathbf{r},\mathbf{r}';E_F)\overleftrightarrow{\partial}_z \sigma^\beta G^A(\mathbf{r}',\mathbf{r};E_F)]\mu_\beta(\mathbf{r}'), \quad (10)$$

where $C = (m_e/\hbar^2)^2 l_m$ is a normalization factor, and l_m the mean free path. By using calculations similar to those leading to Eqs. (8) and (9), the backflow spin current across an interface is

$$\mathbf{j}_z^{\rm back}(0^-) = -\frac{\hbar}{2m_e k_F}\Gamma^0 \mathcal{A}_2 \cdot \boldsymbol{\mu}(0^+), \quad (11)$$

$$\mathbf{j}_z^{\rm back}(0^+) = -\frac{\hbar}{2m_e k_F}\Gamma^0 \mathcal{A}_1 \cdot \boldsymbol{\mu}(0^+). \quad (12)$$

By combining currents due to the spin pumping, backflow, and diffusive current in the NM layer we finally arrive at the spin-pumping current for the FM/NM bilayer. In the NM layer

$$\mathbf{j}_z(z>0) = \frac{\hbar\Gamma^0}{4\pi}\frac{J_{\rm ex}^2}{J_{\rm ex}^2+\Delta^2} N(z)\mathcal{A}_N \cdot \left(\mathbf{m}\times\frac{d\mathbf{m}}{dt}\right), \quad (13)$$

where $N(z) = \sinh[(t_N - z)/\lambda_{\rm sd}]/\sinh(t_N/\lambda_{\rm sd})$; in the FM layer

$$\mathbf{j}_z(z<0) = \frac{\hbar\Gamma^0}{4\pi}\frac{J_{\rm ex}^2}{J_{\rm ex}^2+\Delta^2} F(z)\mathcal{A}_F \cdot \left(\mathbf{m}\times\frac{d\mathbf{m}}{dt}\right), \quad (14)$$

where $F(z)$ is 1 at $z=0$ and has an oscillatory decay in the FM layer. The matrices $\mathcal{A}_N$ and $\mathcal{A}_F$ are

$$\mathcal{A}_N = \frac{1}{1+\xi}\begin{pmatrix} 1-2\eta & 0 & 0 \\ 0 & 1-2\eta & 0 \\ 0 & 0 & 1-3\eta-\frac{\xi\eta}{1+\xi} \end{pmatrix};$$

$$\mathcal{A}_F = \frac{1}{1+\xi}\begin{pmatrix} 1+4\eta\xi & 0 & 0 \\ 0 & 1+4\eta\xi & 0 \\ 0 & 0 & 1+8\eta\xi+\frac{\eta}{1+\xi} \end{pmatrix},$$

where the *backflow factor* $\xi = (3/2)(\Gamma^0/k_F^2)(\lambda_{\rm sd}/l_m)\times \coth(t_N/\lambda_{\rm sd})$ ranges between zero and infinity. $\xi = 0$ refers to the case where there is no backflow; then $\mathcal{A}_F$, $\mathcal{A}_N$ reduce to $\mathcal{A}_1$, $\mathcal{A}_2$. $\xi = \infty$ indicates that the entire spin current pumped into the NM bulk flows back across the interface; then $\mathcal{A}_N$ vanishes and $\mathcal{A}_F$ is proportional to η which means that the entire spin current is relaxed at the interface.

Equations (13) and (14) are our main results. In Fig. 1, we show the spin current in the FM/NM bilayer for various values of the disorder, SOC strength, and thickness of the NM layer. We conclude by discussing the salient features of the dependence of spin pumping on these parameters and relate our results to existing data.

(1) Spin-memory loss and spin-current absorption at interfaces.—The loss of spin current at Cu/Pt interfaces was proposed more than a decade ago. Kurt *et al.* [17] observed in their CPP GMR study that the spin current across a Cu/Pt interface is not continuous. More quantitatively, if the standard spin-diffusion equations are used to fit the data

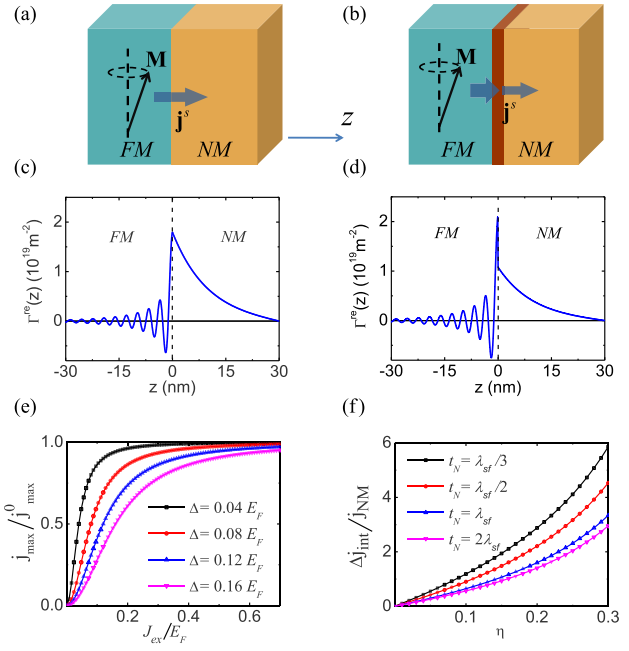

FIG. 1 (color online). Illustration of spin pumping (a) without and (b) with Rashba SOC at the interface. In both cases, (c) and (d), the spin current decays oscillatorily within the FM layer and exponentially in the NM. The maximum spin current $j_{\max}$ occurs at $z = 0^-$. The dependence of $j_{\max}$, normalized to its disorder-free value $j^0_{\max}$, on the ferromagnetic exchange constant for several values of the disorder parameter Δ, (e), where Δ is the imaginary part of self-energy. The ratio of the interface spin-current jump $\Delta j_{\rm int}$ to the spin current relaxed in the NM layer as a function of the SOC strength for several thickness of the NM layer, (f) (in-plane spin polarization).

of magnetoresistance, a spin-memory loss parameter, as large as 90%, at the Cu/Pt interface has to be introduced. The spin-memory loss cannot be due to strong spin-flip scattering in the Pt layer since the measured spin-diffusion length of Pt remains relatively long at 14 nm. We consider such spin-memory loss as the experimental evidence of the strong interfacial SOC. Another experimental support of the loss of spin current at interfaces is the observation that enhanced damping due to spin pumping saturates at just a few monolayers of Pt grown on FM films [8]; i.e., a thicker Pt layer does not increase the damping since the spin current is mainly lost to the interface. These experiments support our idea that the SOC at interfaces absorbs a significant portion of the spin current; quantitative estimates for the loss are determined from Eqs. (13) and (14) as long as the Rashba coefficient is known.

(2) Dependence of the spin current on disorder.—Yoshino *et al.* have investigated the dependence of the enhanced damping on the composition of the ferromagnetic alloy Fe_xNi_{1-x} [31]. It was found that the induced electric voltage scales with the average saturation magnetization of the alloy. In our sd model, the saturation magnetization is proportional to the exchange parameter $J^2_{\rm ex}$, and thus the spin pumping current, Eqs. (13) and (14), which is proportional to the enhanced damping parameter, does predict such dependence in the limit of a strong disorder. In the previous spin-pumping theory [15], the mixing conductance is independent of the alloy composition.

(3) Resolving the controversy between short and long spin diffusion length.—Currently there is a lively debate on the spin-diffusion length of Pt [6–11]. In ferromagnetic resonance experiments, the thickness dependence of the damping constant leads to a short length, typically a few monolayers, while the inverse spin-Hall effect presages a much longer spin-diffusion length for Pt. This discrepancy is resolved by noting that the damping enhancement is mainly associated with absorption of spin current at the interface, while the inverse spin-Hall effect measures the spin current in the bulk of the Pt layer. Our formalism, Eqs. (13) and (14), provides a natural explanation for the different length scales found from different experiments.

(4) Anisotropy of enhanced damping.—Another prediction from Eqs. (13) and (14) is the anisotropy of the pumping current depending on whether the axis for the precessing magnetization is in or perpendicular to the plane of a layer. If we define the enhanced damping parameter as the loss of spin current at the interface and in the NM bulk, we find,

$$\alpha_\perp \propto \frac{1+4\eta\xi}{1+\xi}, \tag{15}$$

$$\alpha_\parallel \propto \frac{1+6\eta\xi}{1+\xi} + \frac{\eta}{2(1+\xi)^2}. \tag{16}$$

The in-plane damping is always larger than the out-of-plane damping. Early experiments overlooked this anisotropy. In Fig. 2, we show the anisotropy of the enhanced damping as the parameters are varied.

(5) Inverse spin Hall from the FM layer.—Equation (14) explicitly determines the spin current in the FM layer. We are unable to analytically write down the expression for the position dependence of $F(z)$ due to different Fermi surfaces in different materials. However, we can estimate the average spin current, $I^t_F \equiv (1/t_{\rm FM})\int_{-\infty}^0 dz\mathbf{j}(z)$, in the FM layer by approximating $F(z)$ as an oscillatory decaying function with a period of $L_{\rm co}=2\pi/(k_{F\uparrow}-k_{F\downarrow})$; it follows that $I^t_F \approx L_{\rm co} j(0^-)$. The inverse spin Hall in the FM layer converts the spin current into a voltage proportional to I^t_F. Such a voltage has recently been observed in NiFe/YIG bilayers [4].

Finally, we wish to comment that our theory may also be applied to study the spin pumping in ferromagnetic and topological insulator bilayers. A spin-pumping-induced robust spin-Hall voltage has already been observed in NiFe/Ag/Bi [2] and NiFe/BiSbTeSe [3]. A possible explanation is that the spin pumping induces a large spin accumulation near the surface of the topological insulator, and a conversion between the spin accumulation and electric current occurs at the momentum-spin-locked surface [32]. We point out that a more quantitative treatment of spin accumulation and induced current on the surface of TI's would have to include the coupling between the

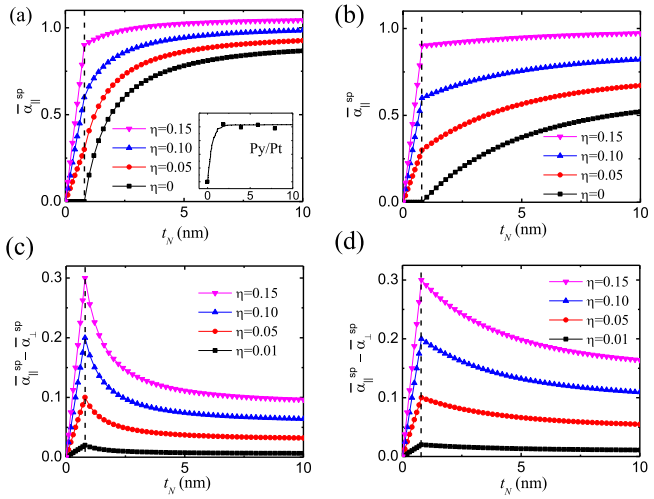

FIG. 2 (color online). The enhanced damping parameter and its anisotropy of spin pumping for several different SOC parameters. (a) The precessing axis is parallel to the layers with the backflow fraction at large NM thickness $\epsilon \equiv \xi/(1+\xi) = 10\%$, and (b) $\epsilon = 40\%$. The dashed lines indicate the effective thickness of the interface. (c) The difference of the enhanced damping parameter for the precessing axis perpendicular and parallel to the layers for $\epsilon = 10\%$, and (d) $\epsilon = 40\%$. The inset in (a) is from the experimental data in Ref. [8].

two-dimensional TI states and three-dimensional metallic states; this requires a separate study.

In summary, we have developed a spin-pumping formalism in the presence of the SOC at the interface. The position dependent spin-pumping current as well as the backflow are analytically expressed in terms of the conventional retarded Green's functions. We have applied the formalism to resolve some long-standing issues on the conflicting conclusions about the spin-diffusion length, and the origin of spin-memory loss at interfaces with heavy metals. We also predict some unanticipated spin-pumping phenomena.

The authors thank Peter M. Levy of New York University for helpful discussions and critical reading of the manuscript. This work is supported by National Science Foundation (Grant No. ECCS-1127751 and 1404542).

*zhangshu@email.arizona.edu

[1] R. Urban, G. Woltersdorf, and B. Heinrich, Phys. Rev. Lett. **87**, 217204 (2001).
[2] J. C. R. Sánchez, L. Vila, G. Desfonds, S. Gambarelli, J. P. Attané, J. M. De Teresa, C. Magén, and A. Fert, Nat. Commun. **4**, 2944 (2013).
[3] Y. Shiomi, K. Nomura, Y. Kajiwara, K. Eto, M. Novak, K. Segawa, Y. Ando, and E. Saitoh, Phys. Rev. Lett. **113**, 196601 (2014).
[4] P. Hyde, L. Bai, D. M. J. Kumar, B. W. Southern, C.-M. Hu, S. Y. Huang, B. F. Miao, and C. L. Chien, Phys. Rev. B, **89**, 180404(R) (2014).
[5] D. Wei, M. Obstbaum, M. Ribow, C. H. Back, and G. Woltersdorf, Nat. Commun. **5**, 3768 (2014).
[6] O. Mosendz, J. E. Pearson, F. Y. Fradin, G. E. W. Bauer, S. D. Bader, and A. Hoffmann, Phys. Rev. Lett. **104**, 046601 (2010).
[7] H. Nakayama, K. Ando, K. Harii, T. Yoshino, R. Takahashi, Y. Kajiwara, K. Uchida, Y. Fujikawa, and E. Saitoh, Phys. Rev. B **85**, 144408 (2012).
[8] Z. Feng, J. Hu, L. Sun, B. You, D. Wu, J. Du, W. Zhang, A. Hu, Y. Yang, D. M. Tang, B. S. Zhang, and H. F. Ding, Phys. Rev. B **85**, 214423 (2012).
[9] V. Vlaminck, J. E. Pearson, S. D. Bader, and A. Hoffmann, Phys. Rev. B **88**, 064414 (2013).
[10] W. Zhang, V. Vlaminck, J. E. Pearson, R. Divan, S. D. Bader, and A. Hoffmann, Appl. Phys. Lett. **103**, 242414 (2013).
[11] M. Obstbaum, M. Härtinger, H. G. Bauer, T. Meier, F. Swientek, C. H. Back, and G. Woltersdorf, Phys. Rev. B **89**, 060407(R) (2014).
[12] K. Ando, S. Takahashi, J. Ieda, H. Kurebayashi, T. Trypiniotis, C. H. W. Barnes, S. Maekawa, and E. Saitoh, Nat. Mater. **10**, 655 (2011).
[13] I. Žutić and H. Dery, Nat. Mater. **10**, 647 (2011).
[14] E. Shikoh, K. Ando, K. Kubo, E. Saitoh, T. Shinjo, and M. Shiraishi, Phys. Rev. Lett. **110**, 127201 (2013).
[15] Y. Tserkovnyak, A. Brataas, and G. E. W. Bauer, Phys. Rev. Lett. **88**, 117601 (2002).
[16] Y. Tserkovnyak, A. Brataas, and G. E. W. Bauer, Phys. Rev. B **66**, 224403 (2002).
[17] H. Kurt, R. Loloee, W. P. Pratt, Jr., and J. Bass, Appl. Phys. Lett. **81**, 4787 (2002).
[18] I. M. Miron, K. Garello, G. Gaudin, P. J. Zermatten, M. V. Costache, S. Auffret, S. Bandiera, B. Rodmacq, A. Schuhl, and P. Gambardella, Nature (London) **476**, 189 (2011).
[19] L. Liu, T. Moriyama, D. C. Ralph, and R. A. Buhrman, Phys. Rev. Lett. **106**, 036601 (2011).
[20] X. Fan, H. Celik, J. Wu, C. Ni, K.-J. Lee, V. O. Lorenz, and J. Q. Xiao, Nat. Commun. **5**, 3042 (2014).
[21] S. Datta, *Electronic Transport in Mesoscopic Systems*, 1st ed. (Cambridge University Press, Cambridge, U.K., 1997).
[22] G. D. Mahan, *Many-Particle Physics*, 3rd ed. (Kluwer Academic/Plenum Publishers, New York, 2000).
[23] See Supplemental Material at http://link.aps.org/supplemental/10.1103/PhysRevLett.114.126602, which includes Refs. [24–27], for detailed derivation of equations in the main text.
[24] M. Trott and Ch. Schnittler, Phys. Status. Solidi B **152**, 153 (1989).
[25] P. M. Levy, H. E. Camblong, and S. Zhang, J. Appl. Phys. **75**, 7076 (1994).
[26] A. Brataas, Y. V. Nazarov, and G. E. W. Bauer, Eur. Phys. J. B **22**, 99 (2001).
[27] H. E. Camblong, P. M. Levy, and S. Zhang, Phys. Rev. B **51**, 16052 (1995).
[28] K. Xia, P. J. Kelly, G. E. W. Bauer, A. Brataas, and I. Turek, Phys. Rev. B **65**, 220401 (2002); X.-T. Jia, K. Liu, K. Xia, and G. E. W. Bauer, Europhys. Lett. **96**, 17005 (2011).
[29] C. R. Ast, J. Henk, A. Ernst, L. Moreschini, M. C. Falub, D. Pacilé, P. Bruno, K. Kern, and M. Grioni, Phys. Rev. Lett. **98**, 186807 (2007).
[30] M. D. Stiles and A. Zangwill, Phys. Rev. B **66**, 014407 (2002).
[31] T. Yoshino, K. Ando, K. Harii, H. Nakayama, Y. Kajiwara, and E. Saitoh, Appl. Phys. Lett. **98**, 132503 (2011).
[32] K. Shen, G. Vignale, and R. Raimondi, Phys. Rev. Lett. **112**, 096601 (2014).